PERGAMON

International Journal of Heat and Mass Transfer 44 (2001) 2209–2223

International Journal of HEAT and MASS TRANSFER

www.elsevier.com/locate/ijhmt

Calibrating for viewing angle effect during heat transfer measurements on a curved surface

T.L. Chan [a,*], S. Ashforth-Frost [b], K. Jambunathan [b]

[a] *Department of Mechanical Engineering, The Hong Kong Polytechnic University, Hung Hom, Kowloon, Hong Kong*
[b] *Department of Mechanical and Manufacturing Engineering, The Nottingham Trent University, Nottingham NG1 4BU, UK*

Received 10 December 1999; received in revised form 10 August 2000

Abstract

Liquid crystal thermography (LCT) has been widely used for the determination of surface heat transfer distribution. However, this technique is sensitive to illumination and viewing angle and therefore limited to surfaces with only slight curvature. A liquid crystal calibration technique using true-colour image processing system has now been developed to alleviate the effect of viewing angle on oblique/curved surfaces. Application of the calibration and transient liquid crystal thermographic techniques and uncertainty analysis to a heated air slot jet impinging on a semi-cylindrical convex surface has been demonstrated. It is shown that the local heat transfer coefficient may be overestimated by up to 39.1% at a viewing angle of 69° from the normal under test conditions. However, the overall uncertainty in heat transfer coefficient can be significantly reduced from the maximum value of 36.3% to within 11.1% by using the implemented viewing calibration technique.

Keywords: Thermochromic liquid crystals; Calibration technique; Viewing angle; Jet impingement heat transfer; Curved surface

1. Introduction

Liquid crystal thermography (LCT) has been widely used for the visualization and determination of surface temperature distributions leading to convective heat transfer coefficients. In recent years, colour image processing has been used to obtain qualitative and quantitative temperature information from surfaces coated with thermochromic liquid crystals (TLCs), from which convective heat transfer coefficients can be inferred. However, the technique is sensitive to illumination and viewing angle and therefore limited to surfaces with only slight curvature. Most of the applications have involved flat surfaces, but a limited number of works have reported that small changes in viewing and/or illumination angle can have a significant effect on the chromatic interpretation of the liquid crystal isotherm [1–4].

The aim of this work is to quantify the effect of viewing angle when the light source and recording video camera (on the same axis) are displaced up to 72° from the normal in the present thermochromic liquid crystal calibration set-up. To facilitate the present study, a liquid crystal calibration system previously developed by Chan et al. [5], using true-colour image processing system, has now been extended to investigate the heat transfer distribution of a heated air slot jet impinging on a oblique/curved surface. Details of the bibliographical works on jet impingement on oblique surface can be referred to Chan et al. [6,7].

2. Thermochromic liquid crystal calibration system

2.1. Thermochromic liquid crystals

Thermochromic liquid crystals have in recent years been widely used in surface heat transfer measurements. In general, the liquid crystal technique is non-intrusive, inexpensive and capable of high spatial resolution and accuracy in temperature measurement. However, the

* Correspondence author. Tel.: +852-2766-6656; fax: 852-2365-4703.
E-mail address: mmtlchan@polyu.edu.hk (T.L. Chan).

0017-9310/01/$ - see front matter
PII: S0017-9310(00)00267-2

Nomenclature

a, b, c, d, e, f, g, h	constant coefficients in Eq. (8)
Bi	Biot number
CCD	charge-coupled device
c	specific heat capacity of acrylic specimen
erf	Gaussian error function
h	local heat transfer coefficient
HSI/H, S, I	hue, saturation, intensity
k	thermal conductivity of acrylic specimen
L	slot nozzle length
Nu_0	stagnation Nusselt number $(= hW/k)$
Nu_S	local circumferential Nusselt number $(= hW/k)$
PAL	phase alternation line
R	radius of the semi-cylindrical convex surface specimen
R30C5W	red start 30°C , blue start 35°C; the other colours exhibit between these 5°C bandwidths
Re_W	Reynolds number of slot jet width at nozzle exit $(= U_j W/v)$
RGB	red, green and blue primaries
S	circumferential distance around a semi-circular convex surface from the centreline of a slot jet
t	time
T	temperature
T_j	mean jet exit temperature
T_{amb}	initial wall (ambient) temperature
$T_{(0,t)}$	local wall temperature at specific time (t)
U_j	slot nozzle exit velocity
W	slot nozzle width
y	thickness of acrylic specimen
Y	slot jet-to-impingement surface distance

Greek symbols

α	thermal diffusivity of acrylic specimen
$\delta X/\mathrm{d}X$	uncertainty of quantity X, units of X
v	kinematic viscosity of air
ρ	density of acrylic specimen

effect of viewing/illumination angle, optical access and deterioration can cause major problems. Proper calibration procedure is therefore essential. Strictly speaking, all TLCs are cholesteric liquid crystals, which possess a special optically active state and reflect incident light selectively over a specific range of wavelengths (colour). As selective reflection of the liquid crystal is a function of temperature, the liquid crystal colour display can be used as a temperature indicator over a large area. Micrographs of these encapsulated chiral nematic thermochromic liquid crystal mixtures (Hallcrest BM/R30C5W/C17-10) are shown in Fig. 1(a)–(d). The encapsulated TLCs respond to change in colour from red to blue in microscopic view when the temperature is increasing accordingly. The micrographs show the microencapsulated liquid crystals with an average of 10–15 μm in diameter and fall within the manufacturers' specification of 1–30 μm in diameter.

During the last decade, digital image processing techniques have been increasingly applied to interpret surface temperatures from LCT, from which local convective heat transfer coefficients are inferred. The image processing technique eliminates the subjective (human) interpretation of colour and replaces the labour intensive process of data analysis. Surface temperature information can be obtained using either chromatic or monochromatic interpretation. Akino et al. [8] used a set of band-pass optical filters; for a steady liquid crystal thermograph the filters were interchanged until a series of isothermal lines had been obtained. Wang et al. [9] used the full intensity history recorded during an experiment to obtain the surface heat transfer coefficient at selected pixels. Guo et al. [10] used a pixel-by-pixel calibration of the thermochromic liquid crystal coating to determine the film cooling heat transfer and effectiveness on a complicated shaped surface of which the viewing angle effects were taken into account. Several authors [5,11–14] obtained the hue versus temperature relationship using the standard chromaticity diagram based on the RGB decomposition of colour. Many isothermal lines can be obtained from a single liquid crystal colour image. This method is more advantageous than the monochromatic approach in terms of time efficiency, image resolution and suitability for transient phenomena. Reviews on the characteristics of TLCs, their monochromatic interpretation, and available methods of surface temperature/heat transfer measurement and their applications can be found in [3,15–18].

2.2. True colour image processing system

The image acquisition and processing system used in the present investigation is composed of a high resolution 756 (horizontal) × 581 (vertical) pixels CCD video

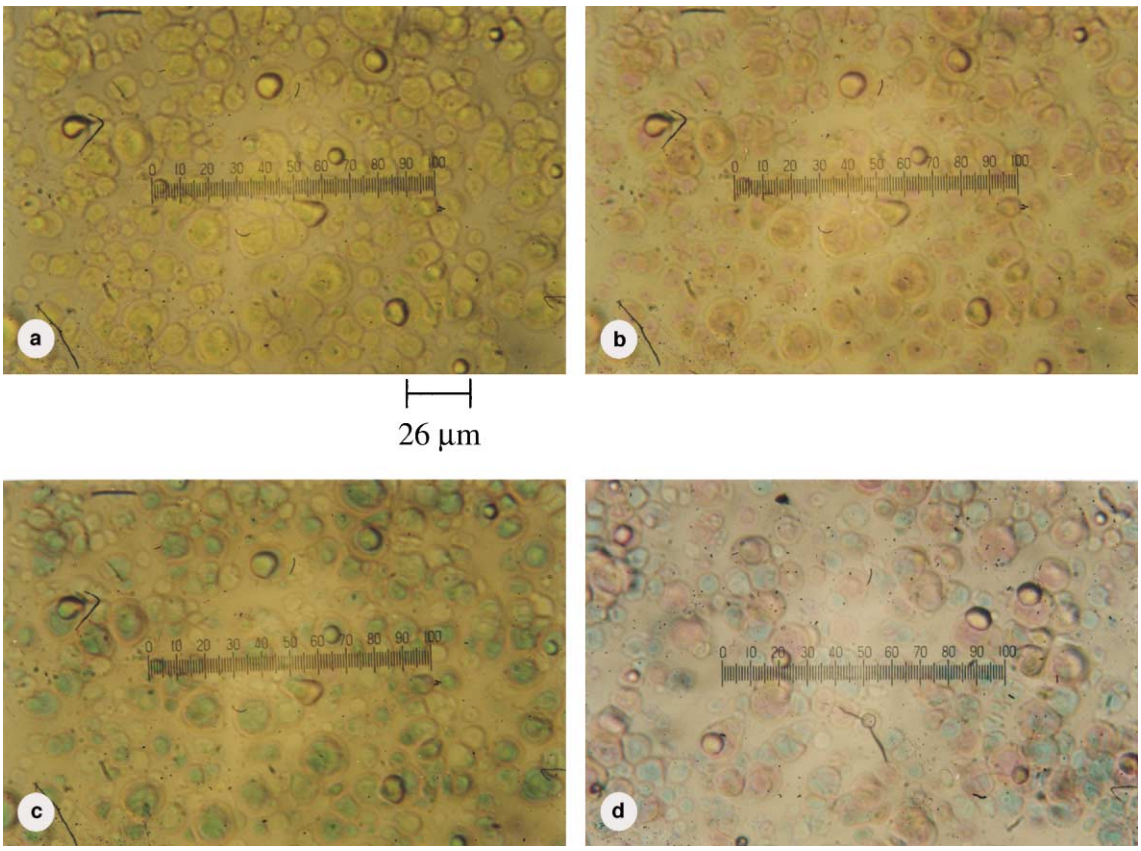

Fig. 1. Microscope photographs of the response of thermochromic liquid crystal (R30C5W).

colour camera (Pulnix TMC-76-PAL) with 12.5 to 75 mm zoom lens (Cosmicar C31204), a colour frame grabber board (Imaging Technology VP-CFG-AT) for 24-bit true colour image processing with 8-bit digitization per colour per pixel, a 16Mb image processing accelerator board (Imaging Technology VIPA-16Mb), a Pentium III personal computer, a Jaz/CD-ROM driver, a professional PAL encoder/decoder compact box for RGB/super-video signal conversion (Truevision VIDI/O Box), a professional PAL super-video cassette recorder (Panasonic AG-7750 Editing SVCR). The use of the zoom lens is to focus and close up the image area of interest by adjusting the focal length between 12.5 and 75 mm without changing the video camera position. However, the focal distance between the video camera and the calibration plate or test specimen must be kept the same.

Only a brief description is given here, the details of colour colorimetric and conversion systems can be found in Chan [5]. In order to enhance the spatial resolution of the colour information, conversion takes place between RGB and PAL super-video signals rather than regular composite video signals. The high quality of super-video signals from the CCD video camera can enhance the twofold spatial resolution of the colour information compared to the regular composite video signals. It can also minimize the signal conversion errors in calibration and experimental work while recording on a high quality super-video cassette when required. The super-video output signals from the CCD video camera are first decoded and then individual red, green, blue and synchronization components of that signal are generated, using the high quality PAL decoder/encoder box. Three digitizers of the image processing board convert the RGB signals into an array of 768×512 pixels by sampling the signal in time, space and intensity. For most colour image processing, the colour description is normally separated from the colour (chrominance) and the intensity (luminance) information. This avoids the generation of colour fringes and users can examine the colour or intensity information closely in their particular application. The RGB format signals are functions of lighting spectral distribution, temperature and filter transmission.

The current 24-bit true-colour image processing board from Imaging Technology, USA is able to transform RGB into HSI and vice versa. The RGB colour model is based on a cube with boundary points at

the 255 scale. It implies that the coordinate points (R, G, B) of eight fundamental colours on the cubical are viewed along the principal diagonal from black and white. This model is normally used to exhibit the colour images in monitors. However, the HSI model is preferred as it can better approximate the human description of colour and is perceptually more uniform than the RGB representation. In addition, hue corresponds to the attribute of a colour perception. Consequently, the colour spectrum information of the TLCs can be more usefully determined. The HSI colour format system can be imagined as a conical shape. Black colour is located at the shape point and white colour is located on the centre of the cone base. The colour image processing and super-video recording system was precalibrated using the standard Macbeth colour checker in the range of 0–255 hue values to be within $\pm 1\%$. Detailed discussion of a colour rendition chart can be referred to [19].

2.3. The lighting system

The choice of different light sources is mainly dependent on their ability to influence the colour appearance of the object. Four common light sources are examined. They are regular fluorescent lamp, metal halide lamp, tungsten lamp and tungsten–halogen lamp/quartz lamp. Millerson [20] described the characteristics of these light sources. The fluorescent lamp produces flicker problems due to the activated AC voltage reverse 100 times a second; the light inherently pulsates. More important still, the quality of fluorescent lighting is not really suitable for an optimal colour reproduction. In fact, the colour rendering of the object under the fluorescent lighting is so unstable that although compensating filters are normally available, many lighting cameramen prefer to turn them off where possible. Metal halide lamps produce a high proportion of ultraviolet light, which is highly undesirable in the liquid crystal application, although an ultraviolet filter is available. Its uneven spectrum of luminance may produce some erroneous colour rendering. The colour and lighting quality of a tungsten lamp deteriorates with use, as its filament evaporates and blackens its bulb. The tungsten–halogen lamp eliminates these problems. In addition, the major benefits of tungsten–halogen lamps are that they produce an excellent colour rendering even in the long run, a reasonably high efficacy, high luminance and compact size as described by de Boer and Fischer [21]. The effect of the lighting/viewing arrangement on the TLCs measurement has been discussed [1,4,22]. Farina et al. [4] reported an uncertainty of ± 0.25°C when an on-axis lighting/viewing arrangement was displaced up to $\pm 25°$ from the normal. However, the liquid crystal temperature shift is much more pronounced when the illuminant is placed off-axis. Chan et al. [22] reported that variations up to -1.3°C were observed for a viewing/illumination angle of 66° from the normal. At 18°, a maximum deviation of -0.6°C occurred which is larger than that observed by Farina et al. [4].

In view of these, a 150 W fibre optics ring light (cold light) source and cross-polarized/filtered CCD video camera lens are used to reduce radiative heating from the light sources to the thermochromic liquid crystals coated surface and ultraviolet light absorbed for the chromatic interpretation. In addition, a better thermochromic liquid crystals calibration technique has been developed to alleviate the significant effect on the chromatic interpretation due to the viewing angle, especially on the curved surfaces.

2.4. Selection of liquid crystal calibration technique

The accurate temperature–colour relationship of liquid crystal material is essential. Such information obtained from the manufacturer is often insufficient. The calibration procedure of liquid crystals can be achieved by a few general methods. Several researchers have used a constant temperature water bath method. The temperature of the bath was monitored and controlled with a temperature controller of up to 0.1°C. The colour of the liquid crystal specimen could be calibrated by increasing the bath temperature in 0.1°C incremental steps throughout the colour spectrum. A thin layer of liquid crystals suspended in a polyacrylate resin was applied to the glass plate, while hot water was circulated on the other side of the plate to obtain a uniform surface temperature, as described by den Ouden and Hoogendoorn [23]. The painted specimen was placed into a sealed clear plastic bag before immersion by Cooper et al. [24]. The working sections were covered with the liquid crystal sheet, while its uniform surface temperature and heat flux were achieved by the water bath, as described by Stasiek et al. [25]. However, to heat up and maintain the new water temperature setting is rather time consuming. Moreover, this method is more suitable for water-proof liquid crystal sheet than the sprayable liquid crystals and black paint products. The latter are usually water soluble, and if these materials are splashed with water or water vapour, these water spots will damage the uniformity of the coating thickness.

A stainless steel foil sheet was used by Hollingsworth et al. [11] to adjust the liquid crystal colour display by varying a small power input to the sheet. The average surface temperature could be determined by the thermocouples, which were attached to the other side of the foil sheet covered with a thick sheet of insulation. However, a uniform surface heat flux is not easy to obtain by using this electrical resistance heating element method.

Several thin foil thermocouples were flush mounted at different locations on the flat heat transfer surface to

determine the temperature–hue calibration data by Camci et al. [12], where the surface was sprayed with black paint and narrow bandwidth liquid crystal material. However, the obtained local surface temperature may not accurately reflect on the hue (in colour) value if the selected image pixel is less than the spot (or size) of thin foil thermocouple.

A linear temperature distribution method was used to determine the temperature–colour relationship of the liquid crystals [8,26]. This technique has been widely used and is probably the most common one. However, Mizell [26] reported the difficulty in maintaining the linearity of the temperature distribution due to changing ambient conditions and the material used for the heat conducting surface.

Based on the above calibration methods and viewing and/or illumination angle problems, a unique calibration technique has been developed for the present investigation on the curved surface. The effect of viewing angle when the light source and recording video camera (on the same axis) are displaced up to 72° from the normal will be discussed in the later section.

2.5. Liquid crystal calibration facility and procedure

The layout of the liquid crystal calibration rig is shown in Fig. 2. A 600 mm long, 160 mm wide and 25 mm thick copper plate was used as the heat conducting surface. The sprayable black backing paint and 5°C bandwidth microencapsulated thermochromic liquid crystal material (BB-G1, BM/R30C5W/C17-10 supplied by Hallcrest, USA) were sprayed uniformly onto a copper conducting surface using a pressurized artist's air brush (Olympos PB-306 and PB-308). A thin layer of thermochromic liquid crystal coating was applied over a water-based black paint, which improves the colour resolution by absorbing unreflected light. The total thickness of the combined layers was estimated to be less than 30 μm with a time response within a few milliseconds by Schultz and Jones [27]. The colour temperature and intensity (Minolta Colour meter III F and Intensity meter III F) of the light source were monitored over the test surface and were observed to be uniform within 3200 ± 10 K and 300 ± 3 lux, respectively. A linear temperature gradient was imposed across the conducting

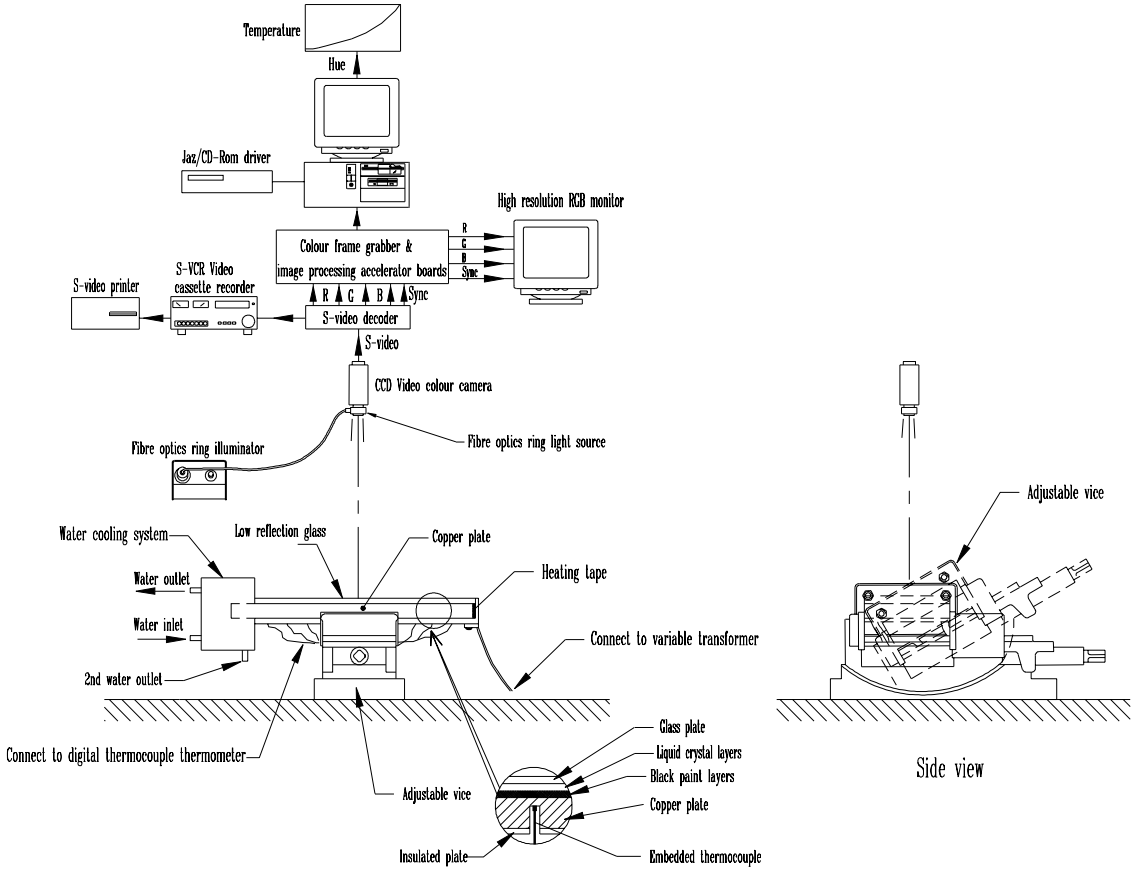

Fig. 2. Schematic diagram of liquid crystal calibration apparatus layout, from Chan et al. [22].

surface using a variable power supply and a constant temperature water bath at opposite sides of the surface, and enclosed beneath was a low-reflectivity optical glass plate with compression springs at four corners of the conducting surface. The low-reflectivity optical glass was used to minimize the overall heat transfer losses in the vertical direction and to ensure the surface temperature varied linearly along the conducting plate. Similar low-reflectivity optical glass was used in Farina's earlier liquid crystal calibration work [4]. The effect of low-reflectivity optical glass on the optical properties of the TLCs is relatively small.

The calibration test surface was illuminated completely by the fibre optics ring light source on-axis lighting/viewing to prevent the ultraviolet and infrared radiation effects and over heating on the coated surface during the TLC calibration process. An adjustable vice facilitated the change in illumination/viewing angle from 0° to 72° in increments of $3° \pm 0.1°$ (SPI-Tronic Pro 360° Digital Level). Nineteen fine-wire Type T thermocouples (0.74 mm diameter and 0.01 second time constant) were embedded in the bottom of the plate to measure the local surface temperature along the conducting surface. All the hue–temperature calibration data were obtained from the seven thermocouples along the centreline of cooper plate. The CCD video camera with zoom lens is placed 1 m away from the middle (i.e. the location of fourth thermocouple) of these seven thermocouples which are 35 mm apart. Therefore, the resulted viewing effect is less than 6° from both ends of the thermocouple from the normal. Earlier work by Farina et al. [4] and the present study have clearly shown that the uncertainty of temperature has found to be relatively insignificant for smaller viewing angle. Hence, it has not been applied in determining the wide-band thermochromic liquid crystal calibration in the present study. The remaining of 12 thermocouples were used to monitor the linearity of surface temperature along the conducting copper plate. All the thermocouples were installed and precalibrated according to Moffat [2]. Temperatures in the range of 30–35°C can be measured within an accuracy of 0.2°C. The location of these thermocouples can be defined on the captured image within the boundary limit of 768 pixels in the horizontal and 512 pixels in the vertical coordinates, respectively. The full colour spectrum of the liquid crystals along the conducting surface can be observed by varying the power supplied to the heating tape as shown in Fig. 3 and is recorded using a CCD video camera with a professional super-video recorder.

A calibration program, developed in Microsoft C language and incorporated into the colour image processing system, was used to capture the hue values at specific pixel locations of the liquid crystal colour displayed along the heat conducting surface and record the corresponding local steady-state surface temperatures output from the thermocouples embedded in the heating plate. Details of calibration program flow chart can be referred to [28]. All input data can be checked and conveniently deleted by this user-friendly software application tool. If any particular hue versus local surface temperature data at specific viewing angle are insufficient, then the calibration procedure can be re-executed.

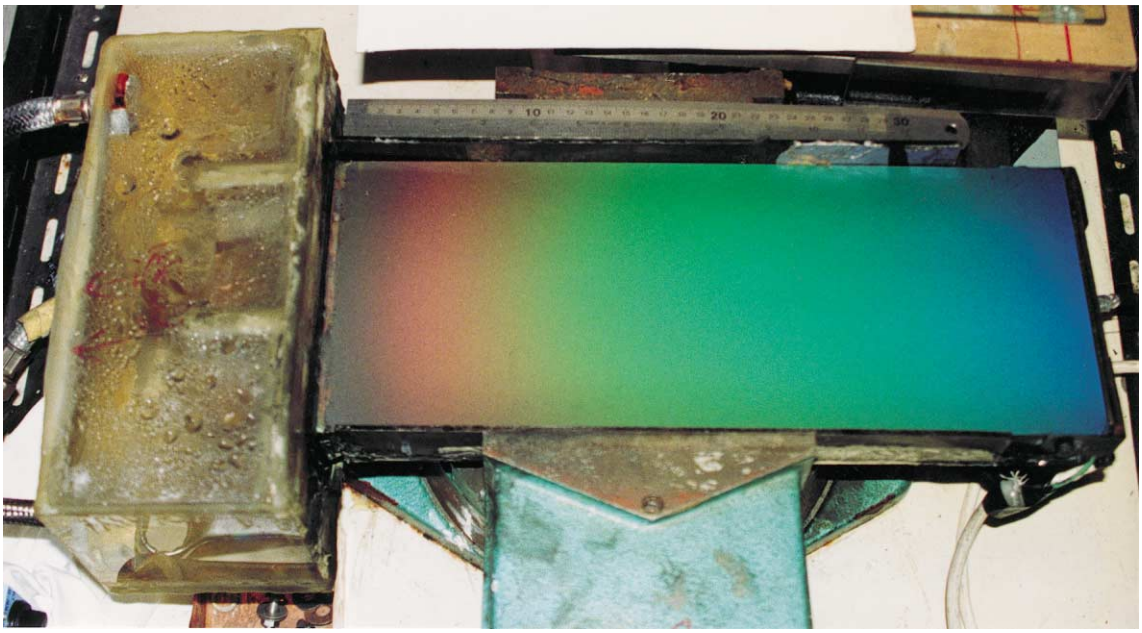

Fig. 3. Photograph of the response of thermochromic liquid crystal colour spectrum along the heat conducting surface.

Nineteen commands (or function keys) of this software program have been developed to fulfill the calibration purpose. For each of the 24 sets of results, more than 500 raw data have been carefully recorded. Ultimately, a graphic representation of the temperature–hue relationship is generated, and the user can observe and note the trend of results immediately.

3. Selection of the heat transfer measurement technique

Two commonly used methods for heat transfer measurement are the steady state, heated-coating liquid crystal method where experimental properties do not vary with time, and the transient liquid crystal method in which heat transfer coefficients are deduced from a time–temperature history recorded. Baughn and Shimizu [29] provided a brief history of these methods. The use of liquid crystals in turbulent heat transfer measurement has been well reviewed [3,17,18]. In general, the heated-coating liquid crystal method provides a better uncertainty in heat transfer coefficient when it is greater than 200 W/m^2 K. Detailed discussions on the comparisons between measurements made with the steady-state, heated-coating and transient liquid crystal methods can be found in [30–32]. But Valencia et al. [33] presented that the corresponding test surface temperature error by the steady (hot film) technique with LCT may be more than 100% when the tangential heat conduction was neglected. In comparison, the transient technique provided less than 20% of its surface temperature difference. Vedula et al. [34] found that the effect of lateral conduction on the determination of local convection heat transfer characteristics with transient tests and surface coatings could be less than 5%. Furthermore, Tarasuk and Castle [35] showed that the electrical power dissipation in a heated wide metallic foil of uniform heater thickness can still be generated 30% higher near the centre of the foil than near the foil edge. On the other hand, the transient technique does not require the maintenance of a uniform surface heat flux especially on a larger surface area and therefore there are less limitations on complex model shapes (i.e. curved surfaces), where such non-uniformities are probable. This transient liquid crystal method has been widely used for very complex geometries, including blade-cooling passages, curved ducts, cylinders, airfoil cooling passages and jet engines [18,36–38]. Based on the above considerations, the transient experimental method was selected for the present investigation.

3.1. Analysis of wall transient technique

This technique requires measurement of the elapsed time to increase the surface temperature of the liquid crystals coated on test acrylic specimen from a known initial temperature to predetermined value. The rate of heating is recorded by monitoring the colour change patterns of the liquid crystal with respect to time. The basic principles and data reduction for transient liquid crystal technique were described by Ireland [39]. If the specimen is made from a material with low thermal diffusivity (i.e. acrylic material) and chosen to be sufficiently thick, then the heat transfer process can be considered to be one-dimensional into a semi-infinite medium. Schultz and Jones [27] suggested a criterion for the minimum thickness of material (y), according to Eq. (1)

$$y > 4\sqrt{\alpha t}, \tag{1}$$

where y is the thickness of specimen, α the thermal diffusivity and t is the time.

The local convective heat transfer is deduced from one-dimensional transient conduction:

$$\frac{T_{(0,t)} - T_{\mathrm{amb}}}{T_{\mathrm{j}} - T_{\mathrm{amb}}} = 1 - \operatorname{erf}\xi - \mathrm{e}^{Bi+\eta}(1 - \operatorname{erf}(\xi + \sqrt{\eta})), \tag{2}$$

where

$$\xi = \sqrt{\frac{y^2}{4\alpha t}}, \quad Bi = \frac{hy}{k} \quad \text{and} \quad \eta = \frac{h^2\alpha t}{k^2} = \frac{h^2 t}{k\rho c}. \tag{3}$$

At the surface, $y = 0$, thus $\xi = Bi = 0$, and Eq. (2) becomes

$$\frac{T_{(0,t)} - T_{\mathrm{amb}}}{T_{\mathrm{j}} - T_{\mathrm{amb}}} = \theta = 1 - \mathrm{e}^{\eta}(1 - \operatorname{erf}\sqrt{\eta}). \tag{4}$$

These Gaussian error function (erf) values can be well evaluated by using the Simpson rule ($\eta \leqslant 9$) and Taylor series ($\eta > 9$).

The Simpson rule can be expressed as follows:

$$\operatorname{erf}\left(\sqrt{\eta}\right) = \frac{2\Delta y}{2\sqrt{\pi}}\left(\exp(-\xi_0^2) + \exp(-\xi_{2m}^2) + 4\sum_{m=1}^{2m}\exp(-\xi_{2m-1}^2) + 2\sum_{m=2}^{2m}\exp(-\xi_{2m-2}^2)\right), \tag{5}$$

and the Taylor series (asymptotic expansion) can be expressed as follows:

$$\operatorname{erf}\left(\sqrt{\eta}\right) = 1 - \frac{1}{\sqrt{\pi\eta}}\mathrm{e}^{-\eta}\left[1 - \frac{1}{2\eta} + \frac{3\cdot 1}{2^2\eta^2} - \cdots - \frac{1\cdot 3\cdot 5\cdot 7\ldots 19\cdot 21}{2^{11}\cdot\eta^{11}}\right]. \tag{6}$$

It is also found that the values of Gaussian error function can be more precise when series expansion for Simpson rule are applied up to 100 terms. However, the computed data processing time will increase almost twofold by using 100 expansion terms instead of 30

terms. Therefore, the 100 expansion terms of Simpson rule are only used in the critical range of $9 \leqslant \eta \leqslant 10.65$. Using the numerical calculation for Gaussian error function, the local heat transfer coefficient can be determined when the local surface temperature information ($T_{(0,t)}$), the jet temperature (T_j), initial ambient temperature (T_{amb}) and the thermal properties of the acrylic specimen are known. Baughn and Shimizu [29] found that the effect of radiation contributes only a maximum of 6% of the uncertainty of the convective heat transfer information which the surface emissivity might vary with the liquid crystal coating thickness. Hence, the radiation correction has not been applied in determining the heat transfer coefficient. A transient program, developed in Microsoft C language is used to calculate the local heat transfer coefficient. Details of the transient program flowcharts are available in [28].

The partial differentiation of the terms of Eq. (4) and the propagation of the uncertainty in each measured variable through this equation are derived from

$$\frac{\partial h}{h} = \left[\left(\frac{\delta t}{2t} \right)^2 + \left(\frac{\delta(\sqrt{\rho ck})}{\sqrt{\rho ck}} \right)^2 + \left(\frac{1}{\beta(T_j - T_{amb})} \right)^2 (\delta T_{(0,t)}^2 + (\theta - 1)^2 \delta T_{amb}^2 + \theta^2 \delta T_j^2) \right]^{0.5},$$

where

$$\beta = 2\sqrt{\eta}[\pi^{-0.5} - \sqrt{\eta}(1 - \theta)]. \quad (7)$$

The uncertainty in h due to $\delta t/2t$ diminishes as t increases and achieves a maximum for higher values of h. The fractional uncertainty in h due to uncertainty in temperature measurement is a minimum when $\beta(T_j - T_{amb})$ is large. Detailed uncertainty analysis can be referred to [40].

4. Results and discussion

In order to assess the effect of viewing angle on the temperature versus hue relationship, and to obtain the thermochromic liquid crystal formulations (R30C5W) calibration over the entire surface, more than 30,000 raw data were recorded and analysed, as shown in Fig. 4(a). Based on a 95% confidence interval, the following generated liquid crystal surface-fit equation (8) was correlated to the collected data:

$$T = a + b \exp\left[-0.5 \left(\frac{V - c}{d} \right)^2 \right] + e \exp\left[-0.5 \left(\frac{H - f}{g} \right)^2 \right] + h \exp\left[-0.5 \left(\left(\frac{V - c}{d} \right)^2 + \left(\frac{H - f}{g} \right)^2 \right) \right]. \quad (8)$$

For the liquid crystals material of R30C5W:

$a = 29.69011$, $b = -0.18971$,
$c = -95.64106$, $d = 204.46378$,
$e = -0.19851$, $f = 282.31227$,
$g = 113.91047$, $h = 18.39552$,

where T, V and H represent temperature, viewing/illumination angle from the normal and hue, respectively. The calibrated liquid crystal temperature with a fitted standard error is less than 0.3°C, $\delta T_{(0,t)}$ based on individual uncertainties inherent to the experimental arrangement, the colour image processing system, the thermocouple and the calibration surface-fit equation. This surface-fit equation was then used to determine the local surface temperatures and heat transfer coefficients of convex surface specimen using the heat transfer transient technique. Fig. 4(b) shows graphically the typical effect of viewing angle on the temperature versus hue characteristics of the liquid crystal (R30C5W) at 0°, 18°, 36°, 54° and 69° . The variations up to −1.3°C at the hue value of 130 were observed for a viewing/illumination angle of 69° from the normal. At about 25°, a maximum deviation of −0.4°C occurred which is slightly larger than that observed by Farina et al. [4].

The CCD video camera was positioned as shown in Fig. 5(a), in which point A is taken as an arbitrary point to calculate its corresponding video camera viewing angle (i.e. $a1 + a3$). The focal distance (BC), 1000 mm of the CCD video camera was fixed at the centre point C, on the 65° angular line as shown in Fig. 5(b). As a result, it can provide a maximum viewing angle of 68.7° at stagnation point O, on the 0° angular line and a minimum viewing angle of 0° at point C, on the 65° angular line for the slot jet impingement heat transfer test arrangement.

The response of TLC surface can be sensitive to the material of TLC, the spraying procedures, coating thickness, deterioration with time and exposure to ultraviolet light. In the present study, the calibration plate was prepared at the same time as the semi-cylindrical surface test specimen to ensure the response of TLCs are consistent by using the same spraying procedures (i.e. black backing paint, the thermochromic liquid crystal material, the pressure setting of air artist's brush spraying, the spray distance to the calibration plate and the test specimen, and the number of spray). A second thermochromic liquid crystal calibration at the end of testing should also be carried out. Negligible change is observed on the performance of thermochromic liquid crystals over several weeks if they are carefully stored in dark, dry and cool conditions. Fig. 4(b) shows that the change of hue with temperature is non-linear on the characteristics of liquid crystal material. Hence, a unique calibration should be performed for any other thermochromic liquid

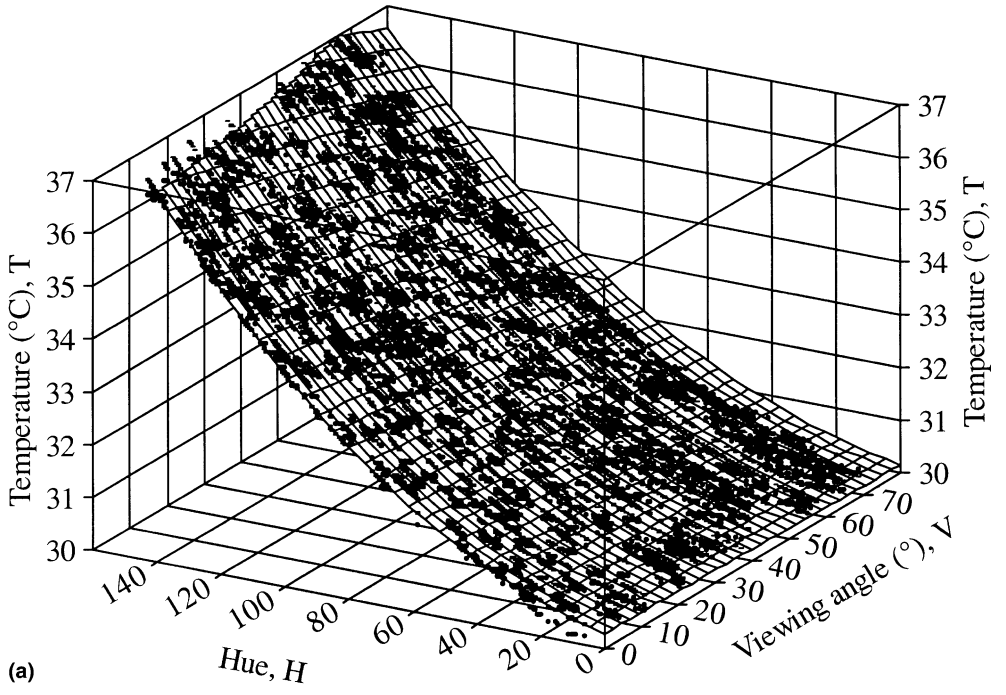

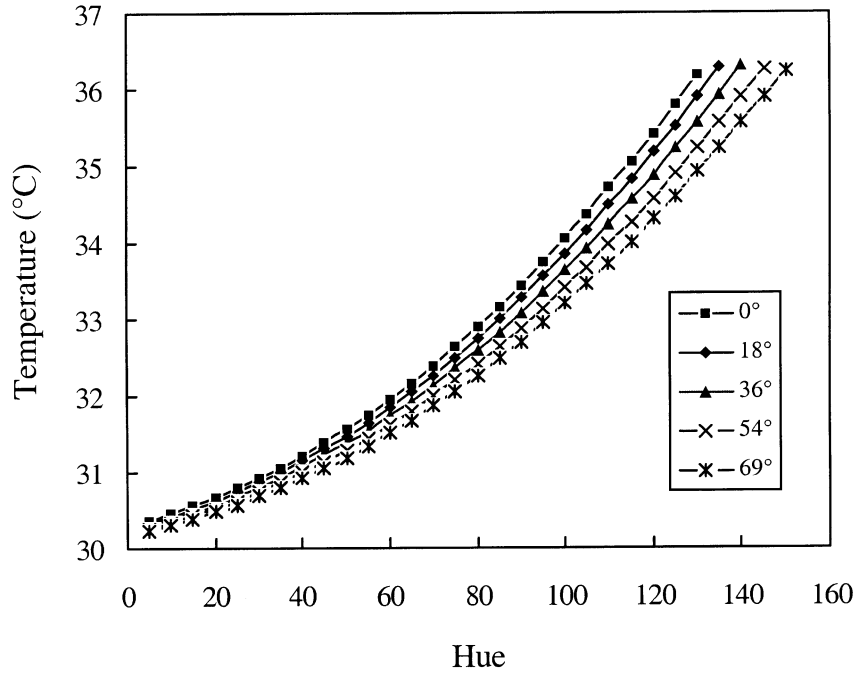

Fig. 4. Thermochromic liquid crystal (R30C5W) calibration results in temperature, hue and viewing angle.

crystal material. Assuming that the liquid crystals will exhibit the same characteristics on the calibration plate and test acrylic specimen under the consistent surface preparation procedures, the above surface-fit equation will allow the surface temperature (and hence heat transfer coefficient) to be determined, with relatively low and known uncertainty, over any oblique surface within the limits of the viewing angle investigated. This will considerably extend the application of the liquid crystal technique to many engineering applications,

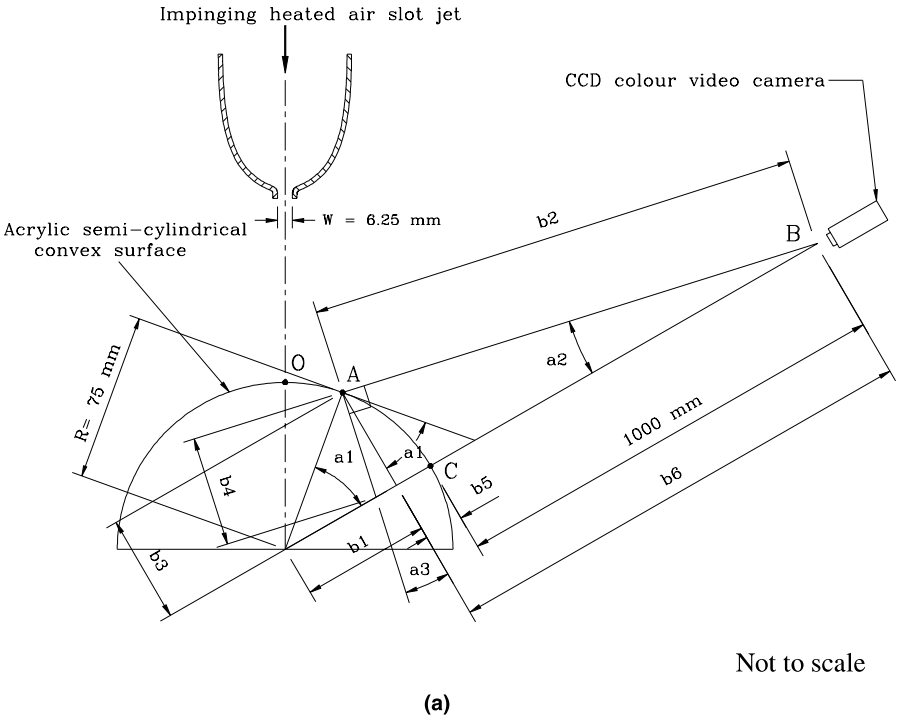

Fig. 5. Schematic diagram of the geometry of video camera viewing angle on a semi-cylindrical convex surface specimen.

both in the laboratory and in situ, where the liquid crystal technique was previously found to be unsuitable due to the orientation or surface curvature.

This viewing calibration technique was incorporated into the transient liquid crystal method to determine the circumferential Nusselt number distribution due to a

heated air slot jet impinging on a semi-cylindrical convex surface for demonstration purpose. The local and global heat transfer coefficients determined by the transient liquid crystal method are independent of the temporal evolution. Fig. 6 shows the comparison between the stagnation Nusselt numbers (Nu_0) of present data and the relevant published correlated data [41] or experimental data [42] available for a slot jet impinging on a convex/flat surface. Nu_0 gradually increases with the dimensionless slot jet-to-impingement surface distance

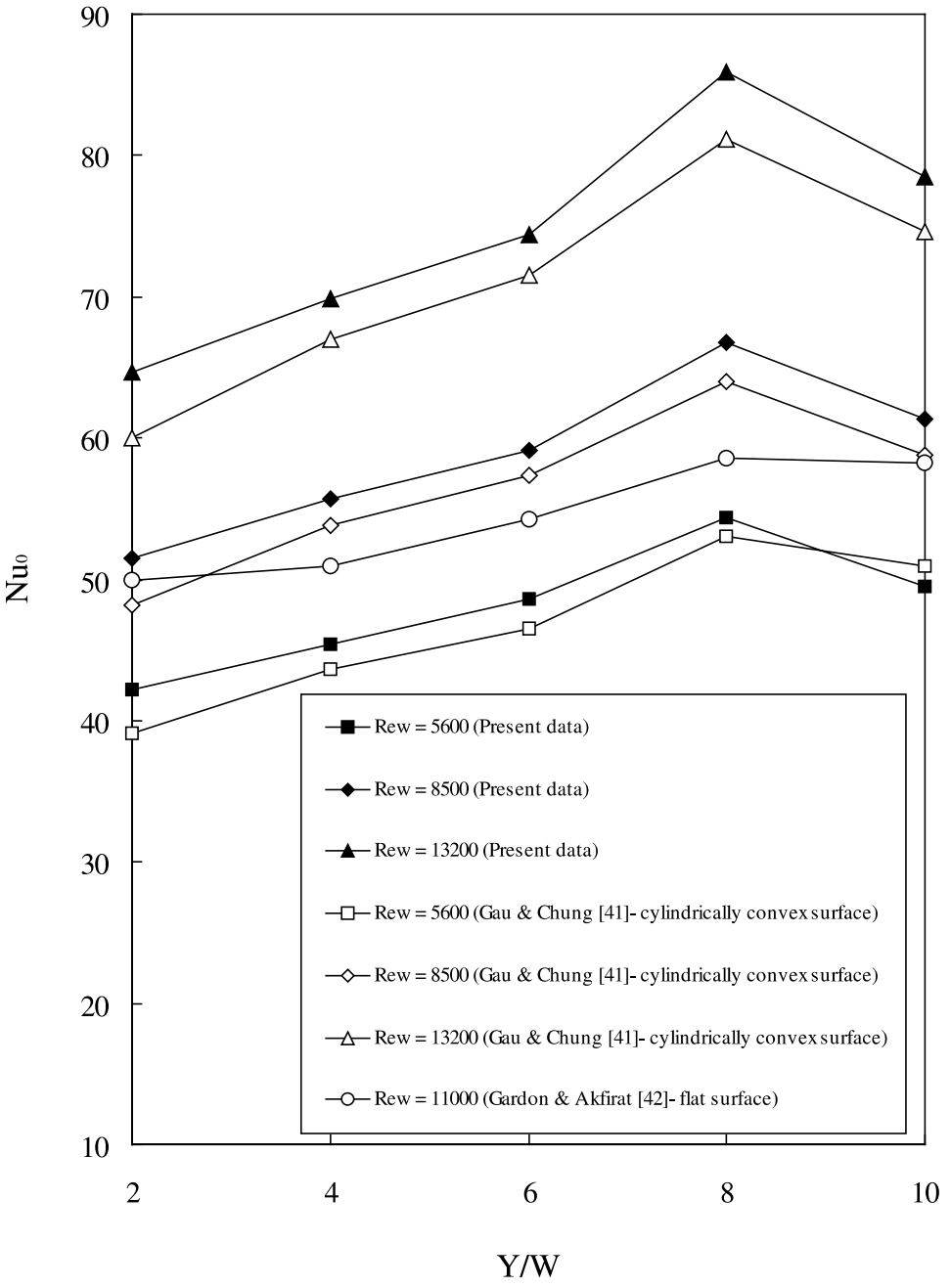

Fig. 6. Comparison of the stagnation Nusselt numbers between present data for a semi-cylindrical convex surface, and the published correlated and experimental data.

(Y/W) and reaches a maximum of $Y/W = 8$. A similar non-linear increase in Nu_0 behaviour with increasing Y/W has also been found [41,42]. The present results have good repeatability and are in agreement with the correlated data obtained from Gau and Chung [41] under similar conditions. The Nu_0 results obtained from Gardon and Akfirat [42] are slightly lower than the present study. Becko [43] stated that a 20% extra correction on their results should be applied due to some experimental errors. Taking account of this experimental correction, a reasonable agreement can be made. Fig. 7 corresponds to increasing the parameter of Y/W from 2 to 10 for a fixed jet Reynolds number of 8500. In general, the local circumferential Nusselt number (Nu_S) decreases from the stagnation point with respect to the parameter of Y/W. For $Y/W = 2$ and 4, the transition starts to take place at $2.7 < S/W < 3.0$ and attains secondary peak (turbulent heat transfer) at $S/W \cong 3.8$. The earlier findings tend to support this similar observation in a different target geometry (i.e. flat, convex cylindrical and hemispherical surfaces) [41,44,45]. When the impingement surface is placed beyond the potential core region, the jet flow arriving at impingement is highly turbulent and mixing due to the influence of the ambient air entrainment. The circumferential Nusselt number distributions are shown in a bell shape and the secondary peak almost disappears due to the stagnation region turbulence effects for $Y/W \geqslant 8$. Subsequent tests have been carried out to fully characterize the circumferential heat transfer distributions associated with this geometry at a range of the dimensionless slot jet-to-impingement surface distance and jet Reynolds numbers in [28].

Fig. 8 shows the effect of viewing angles on the heat transfer coefficients and temperatures under different hue conditions without viewing calibration. It is evident that a serious error in temperature interpretation is identified, with an overestimation of almost 1.3°C at the higher hue value of 130 for the viewing angle of 69° from the normal, but with less influence on the lower hue value of 5. For the higher hue value, the magnitude of error can provide an overestimation of up to 39.1% of the heat transfer coefficient at the viewing angle of 69° from the normal under the test condition. Selection of the test conditions as described leads to the overall uncertainty in heat transfer coefficient from the maximum value of 36.3% to within 11.1% from the selected liquid crystal thermographic image when the video camera viewing angle on the colour interpretation was corrected as shown in Fig. 9.

5. Conclusions

A thermochromic liquid crystal calibration technique has been successfully used to establish a relationship between temperature and hue obtained from recorded liquid crystal images on oblique surface for illumination/viewing angles up to 72° from the normal. This calibration technique has been applied to the uncertainty analysis in a transient liquid crystal thermographic

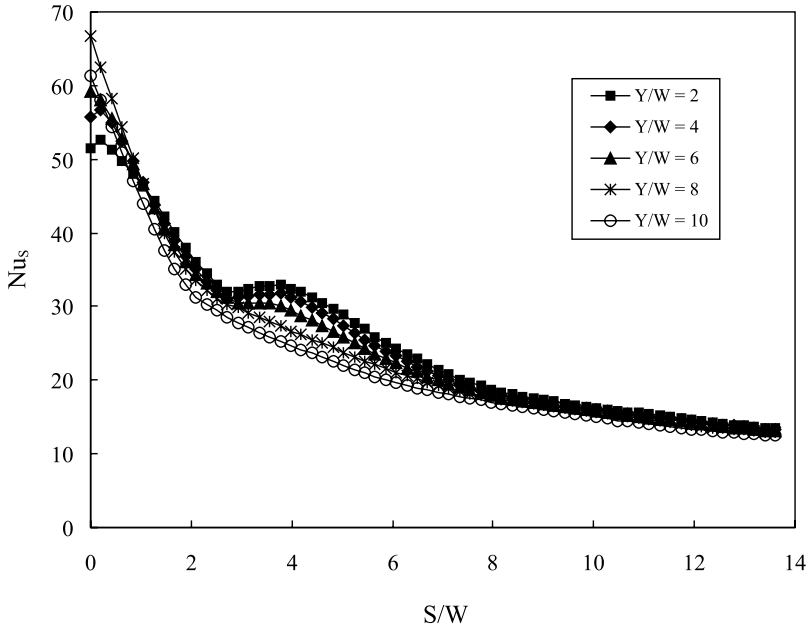

Fig. 7. A typical circumferential Nusselt number distributions for different Y/W on a semi-cylindrical convex surface at $Re_W = 8500$.

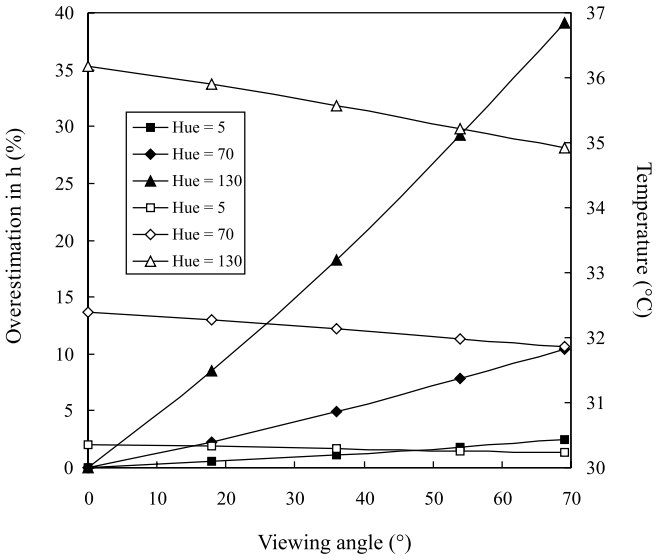

Fig. 8. Effect of viewing angles on the heat transfer coefficients (in solid) and temperatures (in hollow) under different hue conditions without viewing calibration.

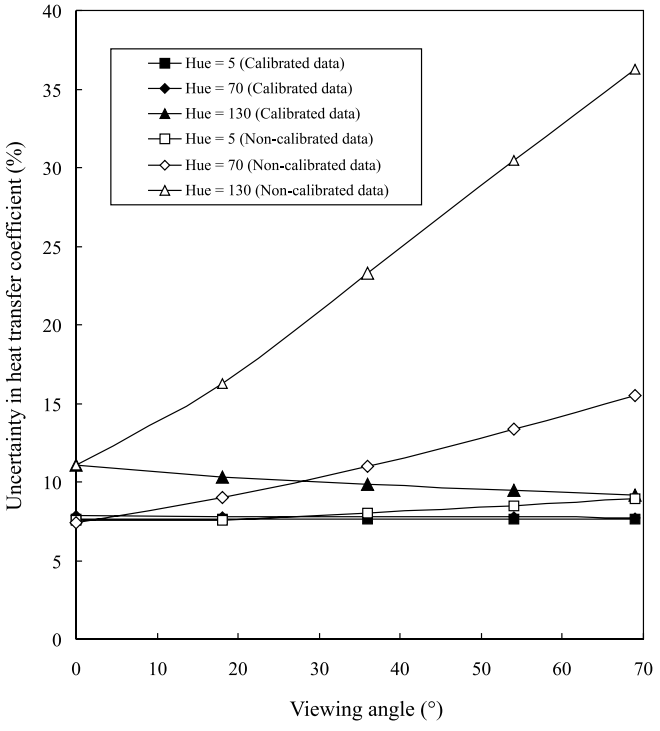

Fig. 9. Effect of viewing angles on the uncertainty in heat transfer coefficients under different hue conditions with and without viewing calibration.

method for the case of a heated air slot jet impinging on a semi-cylindrical convex surface. It has been shown that the maximum overestimation of the heat transfer coefficient at a viewing angle of 69° from the normal can be up to 39.1% under the test conditions. However, it can be reduced significantly from the maximum value of 36.3% to within 11% on the overall uncertainty in heat transfer coefficient by implementing the present calibration technique. Such calibration method will enable the LCT technique to be used more widely in applications where the surface may be non-orthogonal.

Acknowledgements

The first author would like to thank The Hong Kong Polytechnic University for the financial support (Project No. A-PB31) towards this work. We are particularly thankful to the British Council for funding towards travel which helped to strengthen collaboration between the two universities in the early stage.

References

[1] W. Herold, D. Wiegel, Problems of the photographic documentation of liquid crystalline thermographs, in: L. Bata (Ed.), Advances in Liquid Crystal Research and Applications, Pergamon Press, Oxford, 1980, pp. 1255–1259.

[2] R.J. Moffat, Experimental methods for heat transfer studies, Exp. Therm. Fluid Sci. 3 (1990) 14–32.

[3] T.V. Jones, Z. Wang, P.T. Ireland, The use of liquid crystals in aerodynamic and heat transfer experiments, in: Optical Methods and Data Processing in Heat and Fluid Flow, London, 2–3 April 1992, pp. 51–65.

[4] D.J. Farina, J.M. Hacker, R.J. Moffat, J.K. Eaton, Illuminant invariant calibration of thermochromic liquid crystals, Exp. Therm. Fluid Sci. 9 (1994) 1–12.

[5] T.L. Chan, K. Jambunathan, T.P. Leung, S. Ashforth-Frost, A surface temperature calibration method for thermochromic liquid crystals using true-colour image processing, in: Proceedings of the 10th International Heat Transfer Conference, Brighton, UK, 14–18 August 1994, vol. 2, pp. 201–206.

[6] T.L. Chan, K. Jambunathan, S. Ashforth-Frost, Jet impingement on oblique surface – a bibliography: 1870–1977, Previews Heat Mass Transfer 25 (5) (1999) 464–473.

[7] T.L. Chan, K. Jambunathan, S. Ashforth-Frost, Jet impingement on oblique surface – a bibliography: 1978–1998, Previews Heat Mass Transfer 25 (6) (1999) 558–570.

[8] N. Akino, T. Kunugi, K. Ichimiya, K. Mitsushiro, M. Ueda, Improved liquid-crystal thermometry excluding human color sensation, J. Heat Transfer 111 (1989) 558–565.

[9] Z. Wang, P.T. Ireland, T.V. Jones, An advanced method of processing liquid crystal video signals from transient heat transfer experiments, J. Turbomachinery 117 (1995) 184–189.

[10] S.M. Guo, C.C. Lai, J.H. Jeong, T.V. Jones, M.L.G. Oldfield, G.D. Lock, A.J. Rawlinson, Use of liquid crystal techniques to measure film cooling heat transfer and effectiveness, in: AGARD-CP-598, Advanced Non-intrusive Instrumentation for Propulsion Engines, 1997, pp. 20–1 to 20–18.

[11] D.K. Hollingsworth, A.L. Boehman, E.G. Smith, R.J. Moffat, Measurement of temperature and heat transfer coefficient distributions in a complex flow using liquid crystal thermography and true-color image processing, ASME Winter Meeting, San Francisco, CA, 10–15 December 1989, HTD-123, pp. 35–42.

[12] G. Camci, K. Kim, S.A. Hippensteele, A new hue capturing technique for the quantitative interpretation of liquid crystal images used in convective heat transfer studies, ASME Paper 91-GT-122, 1991.

[13] Z. Wang, P.T. Ireland, T.V. Jones, R. Davenport, A color image processing system for transient liquid crystal heat transfer experiments, J. Turbomachinery 118 (1996) 421–427.

[14] H. Babinsky, J.A. Edwards, Automatic liquid crystal thermography for transient heat transfer measurements in hypersonic flow, Exp. Fluids 21 (1996) 227–236.

[15] R.J. Moffat, Experimental methods for heat transfer studies, Exp. Therm. Fluid Sci. 3 (1990) 14–32.

[16] S. Ashforth-Frost, The use of liquid crystals in temperature visualisation, in: Proceedings of Biomechanics '94, Technical University of Wroclaw, Poland, 20–23 October 1994, pp. 342–351.

[17] J.W. Baughn, Review – liquid crystal methods for studying turbulent heat transfer, Int. J. Heat Fluid Flow 16 (1995) 365–375.

[18] P.T. Ireland, A.J. Neely, D.R.H. Gillespie, A.J. Robertson, Turbulent heat transfer measurements using liquid crystals, Int. J. Heat Fluid Flow 20 (1999) 355–367.

[19] C.S. McCamy, H. Marcus, J.G. Davidson, A color rendition chart, J. Appl. Photographic Eng. 11 (3) (1976) 95–99.

[20] G. Millerson, The Technique of Lighting for Television and Film, third ed., Focal Press, UK, 1991, pp. 283–294.

[21] J.B. de Boer, D. Fische, Interior Lighting, Philips Technical Library, Kluwer Technical Books, New York, 1981, p. 147.

[22] T.L. Chan, T.P. Leung, K. Jambunathan, S. Ashforth-Frost, Calibration of thermochromic liquid crystals applied to an oblique surface, in: IMechE Conference Transactions, Fourth UK National Conference on Heat Transfer, Manchester, 26–27 September 1995, pp. 61–66.

[23] C. den Ouden, C.J. Hoogendoorn, Local convective heat transfer coefficients for jets impinging on a plate; experiments using a liquid-crystal technique, in: Proceedings of the Fifth International Heat Transfer Conference, AIChE, 1974, vol. 5, New York, pp. 293–297.

[24] T.E. Cooper, J.F. Meyer, R.J. Field, Liquid crystal thermography and its application to the study of convective heat transfer, ASME Paper No. 75-HT-15, 1975.

[25] J. Stasiek, M.W. Collins, M. Ciofalo, P.E. Chew, Investigation of flow and heat transfer in corrugated passages – I. Experimental results, Int. J. Heat Mass Transfer 39 (1) (1996) 149–164.

[26] L. Mizell, Liquid crystals: a new technique for thermal mapping of electronic components, in: Microelectronics 4:

Fourth International Congress, Munich, 9–11 November 1970, pp. 450–475.
[27] D.L. Schultz, T.V. Jones, Heat transfer measurements in short-duration hypersonic facilities, AGARD 165 (1973).
[28] T.L. Chan, Application of liquid crystal thermography in heat transfer characteristics of slot jet impingement, Ph.D. Thesis, Department of Mechanical and Manufacturing Engineering, The Nottingham Trent University, Nottingham, UK, 1998.
[29] J.W. Baughn, S. Shimizu, Heat transfer measurements from a surface with uniform heat flux and an impingement jet, J. Heat Transfer 111 (1989) 1096–1099.
[30] J.W. Baughn, P.T. Ireland, T.V. Jones, N. Saniei, A comparison of the transient and heated-coating methods for the measurement of local heat transfer coefficients on a pin fin, J. Heat Transfer 111 (1989) 877–881.
[31] C. Whitney, Heat transfer characteristics of slot jet impingement, Ph.D. Thesis, Department of Mechanical Engineering, The Nottingham Trent University, Nottingham, UK, 1996.
[32] S.A. Hippensteele, L.M. Russell, F.S. Stepka, Evaluation of a method for heat transfer measurements and thermal visualization using a composite of a heater element and liquid crystals, J. Heat Transfer 105 (1983) 184–189.
[33] A. Valencia, M. Fiebig, N.K. Mitra, Influence of heat conduction on determination of heat transfer coefficient by liquid crystal thermography, Exp. Heat Transfer 8 (1995) 271–279.
[34] R.P. Vedula, D.E. Metzger, W.B. Bickford, Effects of lateral and anisotropic conduction on determination of local convection heat transfer characteristics with transient tests and surface coatings, Winter Annual Meeting of ASME, Chicago, IL, 27 November–2 December 1988, HTD-I, pp. 21–27.
[35] J.D. Tarasuk, G.S.P. Castle, Temperature distribution in an electrically heated wide metallic foil, J. Heat Transfer 105 (1983) 210–212.
[36] R.J. Clifford, T.V. Jones, S.T. Dunne, Techniques for obtaining detailed heat transfer coefficient measurements within gas turbine blade and vane cooling passages, ASME Paper No. 83-GT-58, 1983.
[37] H.J. Saabas, S.C. Arora, W.A. Messeh, Application of the transient test technique to measure local heat transfer coefficients associated with augmented airfoil cooling passages, ASME Paper No. 87-GT-212, 1987.
[38] C. Camci, K. Kim, S.A. Hippensteele, P.E. Poinsatte, Evaluation of a hue capturing based transient liquid crystal method for high-resolution mapping of convective heat transfer on curved surfaces, J. Heat Transfer 115 (1993) 311–318.
[39] P. Ireland, Internal cooling of turbine blades, Ph.D. Thesis, Department of Engineering Science, University of Oxford, Oxford, UK, 1987.
[40] S.J. Kline, F.A. McClintock, Describing uncertainties in single sample experiments, Mech. Eng. 75 (1953) 3–8.
[41] C. Gau, C.M. Chung, Surface curvature effect on slot-air-jet impingement cooling flow and heat transfer process, J. Heat Transfer 113 (1991) 858–864.
[42] R. Gardon, J.C. Akfirat, Heat transfer characteristics of impinging two-dimensional air jets, J. Heat Transfer (1966) 101–108.
[43] Y. Becko, Impingement cooling – a review, in: Lecture Series 83, von Karman Institute for Fluid Dynamics, 12–16 January 1976, pp. 1–44.
[44] F.F. Cadek, R.D. Zerkle, Local heat transfer characteristics of two-dimensional impinging air jets theory and experiment, Heat Transfer 11 (1974) 15–19.
[45] D.H. Lee, Y.S. Chung, D.S. Kim, Turbulent flow and heat transfer measurements on a curved surface with a fully developed round impinging jet, Int. J. Heat Fluid Flow 18 (1997) 160–169.